

Exposure to extremely low-frequency electromagnetic fields inhibits T-type calcium channels via AA/LTE₄ signaling pathway[☆]



Yujie Cui, Xiaoyu Liu, Tingting Yang, Yan-Ai Mei, Changlong Hu*

School of Life Sciences, Institutes of Brain Science and State Key Laboratory of Medical Neurobiology, Fudan University, Shanghai 200433, China
Open access under CC BY-NC-SA license.

ARTICLE INFO

Article history:

Received 19 August 2013

Received in revised form 26 October 2013

Accepted 27 November 2013

Available online 5 December 2013

Keywords:

Extremely low-frequency electromagnetic fields

T-type calcium channels

The cysteinyl leukotrienes

ABSTRACT

Extremely low-frequency electromagnetic fields (ELF-EMF) causes various biological effects through altering intracellular calcium homeostasis. The role of high voltage-gated (HVA) calcium channels in ELF-EMF induced effects has been extensively studied. However, the effect of ELF-EMF on low-voltage-gated (LVA) T-type calcium channels has not been reported. In this study, we test the effect of ELF-EMF (50 Hz) on human T-type calcium channels transfected in HEK293 cells. Conversely to its stimulant effects on HVA channels, ELF-EMF exposure inhibited all T-type (Cav3.1, Cav3.2 and Cav3.3) channels. Neither the protein expression nor the steady-state activation and inactivation kinetics of Cav3.2 channels were altered by ELF-EMF (50 Hz, 0.2 mT) exposure. Exposure to ELF-EMF increased both arachidonic acid (AA) and leukotriene E₄ (LTE₄) levels in HEK293 cells. CAY10502 and bestatin, which block the increase of AA and LTE₄ respectively, abrogated the ELF-EMF inhibitory effect on Cav3.2 channels. Exogenous LTE₄ mimicked the ELF-EMF inhibition of T-type calcium channels. ELF-EMF (50 Hz) inhibits native T-type calcium channels in primary cultured mouse cortical neurons via LTE₄. We conclude that 50 Hz ELF-EMF inhibits T-type calcium channels through AA/LTE₄ signaling pathway.

© 2013 The Authors. Published by Elsevier Ltd. All rights reserved.

1. Introduction

Exposure to Extremely low-frequency electromagnetic fields (ELF-EMF) causes various cellular and physiological effects (for reviews, see references [1–3]). Calcium homeostasis has been the focus of biological effects of ELF-EMF, and compelling studies show that calcium plays important roles in ELF-EMF induced various biological effects [4–10]. A number of studies suggested that voltage-gated calcium channels (VGCCs) maybe one of the direct targets of ELF-EMF (for review, see reference [11]). VGCCs include high-voltage-gated [Cav1 family (L-type), Cav2 family (P/Q-type, N-type and R-type)] and low-voltage-gated [Cav3 family (T-type)] calcium channels [12].

Among high-voltage-gated calcium channels, the role of L-type calcium channels in ELF-EMF (50/60 Hz) induced effects has been well studied. The L-type calcium channel inhibitor nifedipine inhibits ELF-EMF (60 Hz) induced neurite-like growth of rat chromaffin cells, and BayK8644 (an agonist of L-type calcium

channels) promotes ELF-EMF induced neurite-like growth in chromaffin cells [13]. Through increasing L and N-type channel expression, ELF-EMF (50 Hz) promotes proliferation of human neuroblastoma IMR32 and rat pituitary GH3 cell, and reduces IMR32 cell apoptosis induced by puromycin and H₂O₂ [14]. Nimodipine, an L-type channel blocker, inhibits ELF-EMF (60 Hz) induced thermal hyperalgesia in mice [15]. The L-type channel inhibitor nifedipine prevents ELF-EMF (50 Hz) induced differentiation of pituitary AtT20 D16V cells [16]. ELF-EMF (50 Hz) promotes neurogenesis both in vivo and in vitro through enhancing Cav1-channel activity [17,18]. N-type calcium channels are also involved in ELF-EMF induced biological effects [14]. The literature above indicates that ELF-EMF has a stimulant effect on high-voltage-gated calcium channels.

Compared to high-voltage-gated calcium channels, low-voltage-gated T-type calcium channels have unique electrophysiological features of activation at subthreshold voltages, slow deactivation, fast inactivation, and tiny single-channel conductance [12,19,20]. T-type calcium channels, consisting of Cav3.1, Cav3.2 and Cav3.3 subtypes, are widely expressed and play key roles in various physiological and pathological functions such as neuronal burst firing, cardiac pacemaking, secretion of hormones, cardiac hypertrophy, tumor proliferation and epilepsy [19,21,22]. So far, the effect of exposure to ELF-EMF on T-type calcium channels has remained unclear.

In present study, we test whether ELF-EMF (50 Hz) has effect on cloned human T-type calcium channel activity in HEK293 cells,

[☆] This is an open-access article distributed under the terms of the Creative Commons Attribution-NonCommercial-ShareAlike License, which permits non-commercial use, distribution, and reproduction in any medium, provided the original author and source are credited.

* Corresponding author at: School of Life Sciences and Institutes of Brain Science, Fudan University, 220 Handan Road, Shanghai 200433, China. Tel.: +86 21 65643924; fax: +86 21 55664711.

E-mail address: clhu@fudan.edu.cn (C. Hu).

and on T-type calcium channels in primary cultured mouse cortical neurons. Surprisingly, our results showed that conversely to its stimulant effects on L-type calcium channels, ELF-EMF inhibited T-type channel currents. Our results provide the first evidence that: 1) exposure to ELF-EMF increases LTE₄ release from HEK293 cells, 2) Exogenous LTE₄ inhibits T-type calcium channels, and 3) ELF-EMF (50 Hz) exposure inhibits T-type calcium channel via AA/LTE₄ signaling pathway.

2. Materials and methods

2.1. Ethics statement

The study was carried out in strict accordance with the recommendations in the Guide for the Care and Use of Laboratory Animals of the National Institutes of Health. The protocol was approved by the Committee on the Ethics of Animal Experiments of the Fudan University. All surgery was performed under sodium pentobarbital anesthesia, and all efforts were made to minimize suffering.

2.2. Chemicals

Nordihydroguaiaretic acid (NDGA), flufenamic acid (FA), 17-Octadecenoic acid (ODYA), BAYμ9773 and Bestatin were purchased from Sigma-Aldrich (St. Louis, MO, USA); Leukotriene E₄ and CAY10502 were purchased from Cayman Chemical (Ann Arbor, MI, USA).

2.3. Cell culture and transfection

HEK293 (human embryonic kidney cells) cells were purchased from the cell bank of Chinese Academy of Sciences (Shanghai, China). Cells were cultured in Dulbecco's modified Eagle's medium (DMEM, GIBCO) supplemented with 10% fetal bovine serum, 1% antibiotic antimycotic solution (Gibco). Transient transfections with plasmids for human Cav3.1, Cav3.2 (kindly provided by Professor Paula Barrett [23]) and Cav3.3 (kindly provided by Professor Edward Perez-Reyes [24]) channels in pcDNA3 plasmids were performed using jetPRIME reagents (Polyplus-transfection) according to the manufacturer's instructions, and were used for patching or other biochemical tests 24 h after transfection.

Cortical neurons were derived from the cerebral neocortex of 15-day-old embryonic ICR mice as originally described [25]. Isolated cells were then plated onto 35-mm-diameter Petri dishes coated with poly-L-lysine (1 μg/mL) at a density of 1 × 10⁵ cells per dish. The cultured cells were cultured in Dulbecco's Modified Eagle's Medium (DMEM) supplemented with 10% fetal calf serum, 10% heat-inactivated horse serum and a 1% antibiotic-antimycotic solution. All experiments were carried using cortical neurons at 6–10 days in culture.

2.4. Electrophysiology

Whole-cell currents in the HEK293 cells were recorded using an Axopatch 200B or 700B amplifier (Axon Instruments). The bath solution contained (in mM) 143 TEACl, 10 CaCl₂, 2 MgCl₂, 10 HEPES, 10 glucose, pH 7.4 (adjusted with TEAOH). The internal solution contained (in mM) 125 CsCl, 10 HEPES, and 10 EGTA, 1 MgCl₂, 1 CaCl₂, 5 Mg-ATP, 0.3 Tris-GTP (pH adjusted to 7.2 using CsOH). The pipettes were created from capillary tubing (BRAND, Wertheim, Germany) and had resistances of 4–6 MΩ under these solution conditions. All of the recordings were performed at room temperature. Steady-state calcium channel activation was determined by tail currents using the following protocol. The cells were held at -90 mV and depolarized in 5-mV steps from -60 to +15 mV at 10-s intervals upon repolarization to -70 mV. For steady-state channel

inactivation, the cells were tested at -20 mV from a pre-pulse incremented in 5 mV (-85 mV to -30 mV; 10 s) upon repolarization to -70 mV. The currents were sampled at 10 kHz and filtered at 2 kHz, and corrected online for leak and residual capacitance transients using a P/4 protocol.

2.5. Intracellular AA assay

Intracellular AA levels in HEK 293 cells were measured as previously described [26]. Briefly, HEK 293 cells were plated in 35-mm dishes and grown to confluence. Before test, the culture medium was changed to 1 mL DMEM without serum, and cells were exposed to ELF-EMF (50 Hz, 0.2 mT) for 1 h. The medium was then removed, and the cells were lysed using 0.45% NP40. The lysate was centrifuged for 5 min at 4 °C. The supernatant was then collected for AA assay using a direct human AA ELISA kit (R&B, Lianshuo Bio-Tech, Shanghai, China) according to the manufacturer's instructions.

2.6. LTE₄ release assay

LTE₄ levels in the culture media were measured using highly sensitive enzyme-linked immunosorbent assay kits (R&B, Lianshuo Bio-Tech, Shanghai, China) according to the manufacturer's instructions. Briefly, HEK 293 cells were plated in 35-mm dishes and grown to confluence. Before test, the culture medium was changed to 1 mL DMEM without serum and cells were exposed to ELF-EMF (50 Hz, 0.2 mT) for various time (0.5 h, 1 h, 2 h, 3 h). The media were then collected and centrifuged for 5 min at 4 °C. The supernatant was collected and assayed for levels of LTE₄.

2.7. Western blot

Cell homogenates were prepared using HEPES-NP40 lysis buffer (20 mM HEPES, 150 mM NaCl, 0.5% NP-40, 10% glycerol, 2 mM EDTA, 100 μM Na₃VO₄, 50 μM NaF, pH 7.5). The protein samples were resolved using 10% SDS PAGE and transferred to polyvinylidifluoride (PVDF) membranes in a transfer buffer (25 mM Tris, 192 mM glycine, 20% methanol, v/v) at 230 mA for 2 h. The PVDF membranes were blocked with 10% nonfat dry milk in TBST (TBS containing 0.05% Tween 20) for 1 h at room temperature. The membranes were incubated with the primary antibody in TBST with 5% BSA (bovine serum albumin), overnight at 4 °C. The blot was washed 3 times for 10 min in TBST and incubated with a horseradish peroxidase-conjugated secondary antibody (1/50,000) (KangChen Bio-tech) in TBST with 5% nonfat dry milk for 1 h at room temperature. The blots were developed using enhanced chemiluminescence (ECL) reagents from Pierce and the ChemiDoc XRS+ imaging system from Bio-Rad.

2.8. ELF-EMF exposure

The system used to generate electromagnetic fields was the same as previous reported [26]. Briefly, HEK293 cells were exposed to a magnetic field (50 Hz, 0.2 mT) produced by a pair of Helmholtz coils, which were powered by an AC generator system. The geometry of the system assured a uniform field for cell exposure. An EMF sensor connected to a digital multimeter was used to continuous monitor the frequency and density of EMF. All ELF-EMF experiments were done with a frequency of 50 Hz and a density of 0.2 mT. Duration of ELF-EMF exposure, air and culture medium temperatures were continuously monitored, and ELF-EMF (50 Hz, 0.2 mT) did not change the temperature of the CO₂ incubator (37 °C). Non-EMF control groups were placed in the same incubator in which the conditions were the same as for the exposed groups but without EMF.

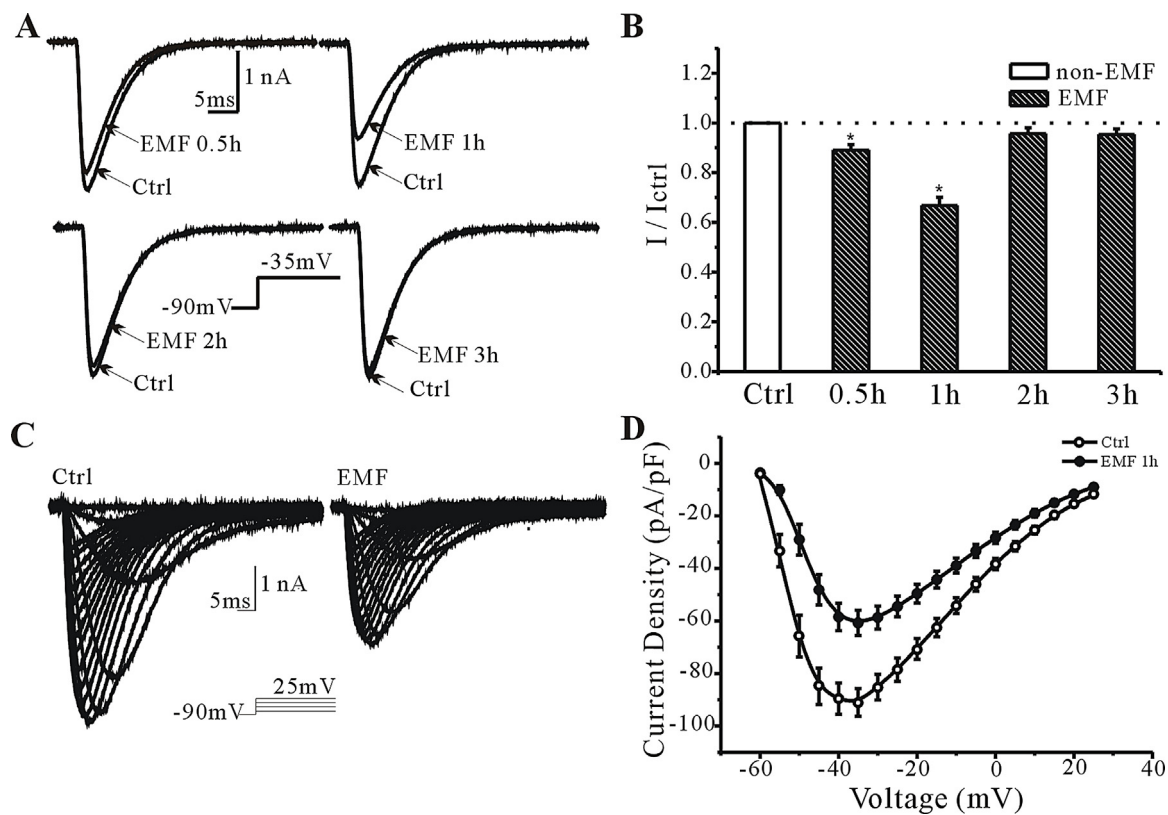


Fig. 1. Exposure to ELF-EMF (50 Hz, 0.2 mT) inhibits Cav3.2 channels in HEK 293 cells. (A) Sample current traces were obtained from HEK293 cells expressed Cav3.2 channels inhibited by exposure to ELF-EMF for different time periods (from 0.5 h to 3 h). (B) Histogram plots of mean \pm S.E.M. of I_{Ca} current density normalized by control ($n=45-60$). * $P<0.05$ compared to control using a one-way ANOVA test. (C) current–voltage (I – V) currents obtained from Cav3.2-transfected HEK293 cells with/without exposure to ELF-EMF for 1 h (50 Hz, 0.2 mT). (D) I – V relationship curves generated by peak current density at each test voltage. Data were presented as means \pm S.E.M. from 50 cells.

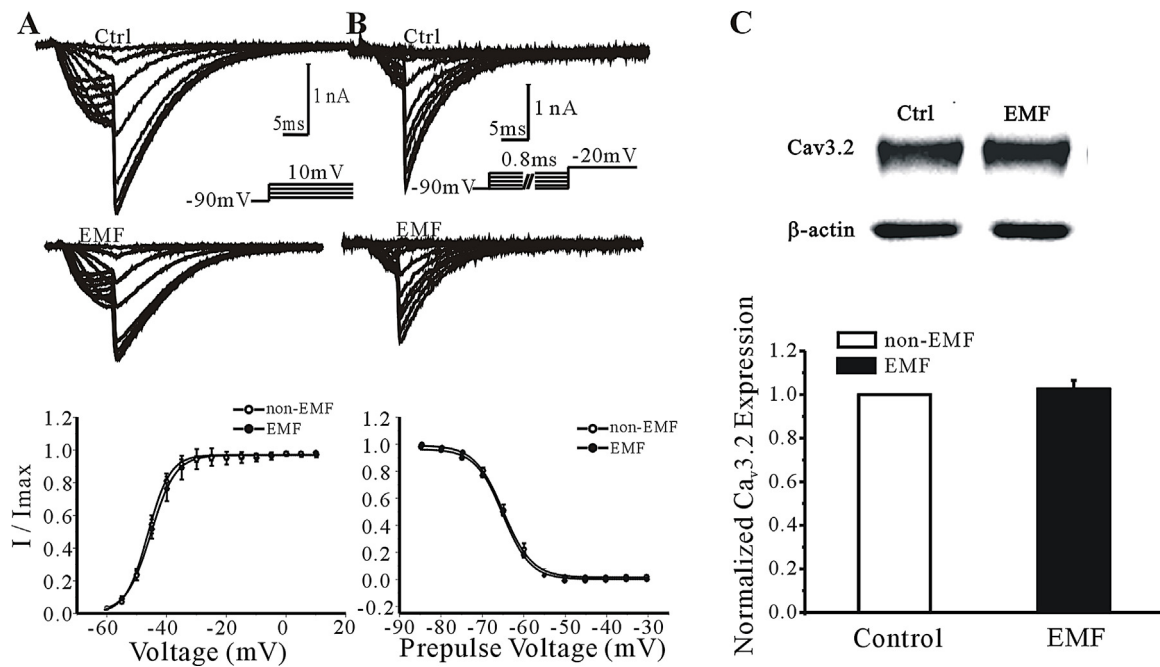


Fig. 2. ELF-EMF exposure did not alter the steady-state activation/inactivation properties and protein expression of Cav3.2. (A) The effect of ELF-EMF exposure for 1 h on the steady-state activation of Cav3.2. The current traces show the voltage-dependent Cav3.2 current activation curves in the absence (top) and presence (middle) of ELF-EMF exposure; the normalized data points were fitted using a Boltzmann equation (bottom). ELF-EMF did not alter the steady-state Cav3.2 activation. (B) The effect of ELF-EMF exposure on the steady-state activation of Cav3.2. The current traces show the voltage-dependent Cav3.2 current inactivation curves in the absence (top) and presence (middle) of ELF-EMF exposure; the normalized data points were fitted using a Boltzmann equation (bottom). ELF-EMF did not change the steady-state Cav3.2 inactivation. (C) 1 h exposure to ELF-EMF did not alter the protein expression of Cav3.2 channels. A representative image (Upper) and the statistical analysis of Western blot from 4 independent experiments (Lower).

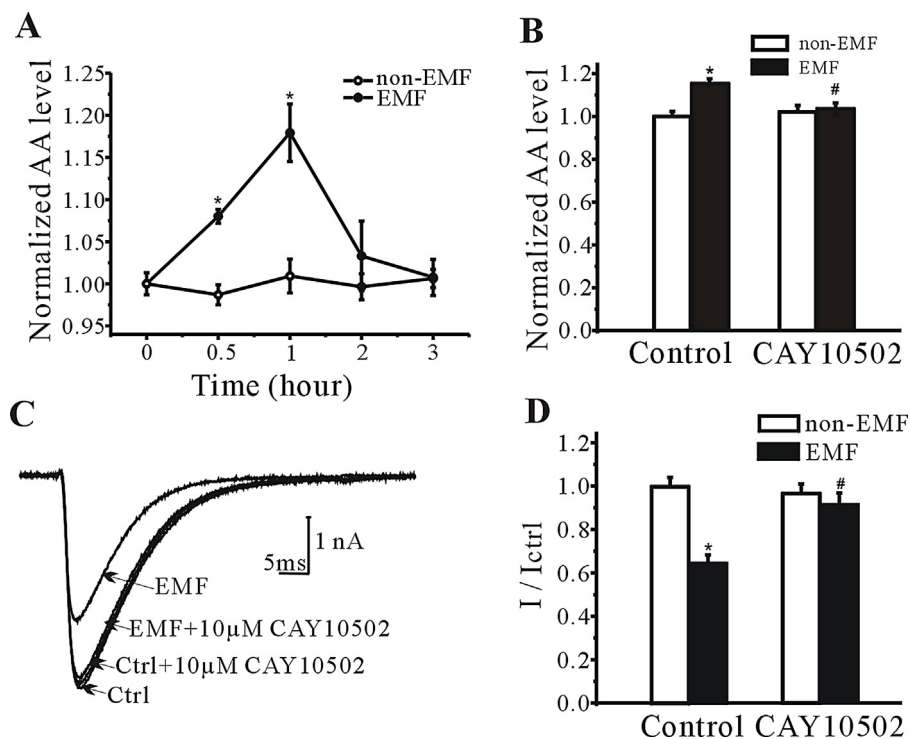


Fig. 3. The ELF-EMF inhibition of Cav3.2 current is mediated by AA. (A) ELF-EMF exposure increased AA concentration in HEK293 cells in a time-dependent manner. (B) The PLA2 inhibitor CAY10502 blocked the EMF (1 h) induced AA increase. The data are from 3 independent experiments. (C) CAY10502 blocked the inhibitory effect of ELF-EMF on CaV3.2 channels. Currents were elicited by a depolarizing pulse to -35 mV from holding at -90 mV. (D) Statistical analysis of the blocking effect of CAY10502 on the ELF-EMF induced inhibition of Cav3.2 channels. * $P < 0.05$ compared to the non EMF-exposed control. # $P < 0.05$ compared to the EMF-exposed group without CAY10502.

2.9. Data analysis

The data analysis was performed with Clampfit 10.3 (Axon Instruments) and Origin 7.5 software (OriginLab). The statistical

analysis consisted of unpaired or paired (depending on the circumstances) Student's *t* tests. Values are given as the means \pm S.E.M, and *n* indicates the number of tested cells or independent test. $P < 0.05$ was defined to be a statistically significant difference between

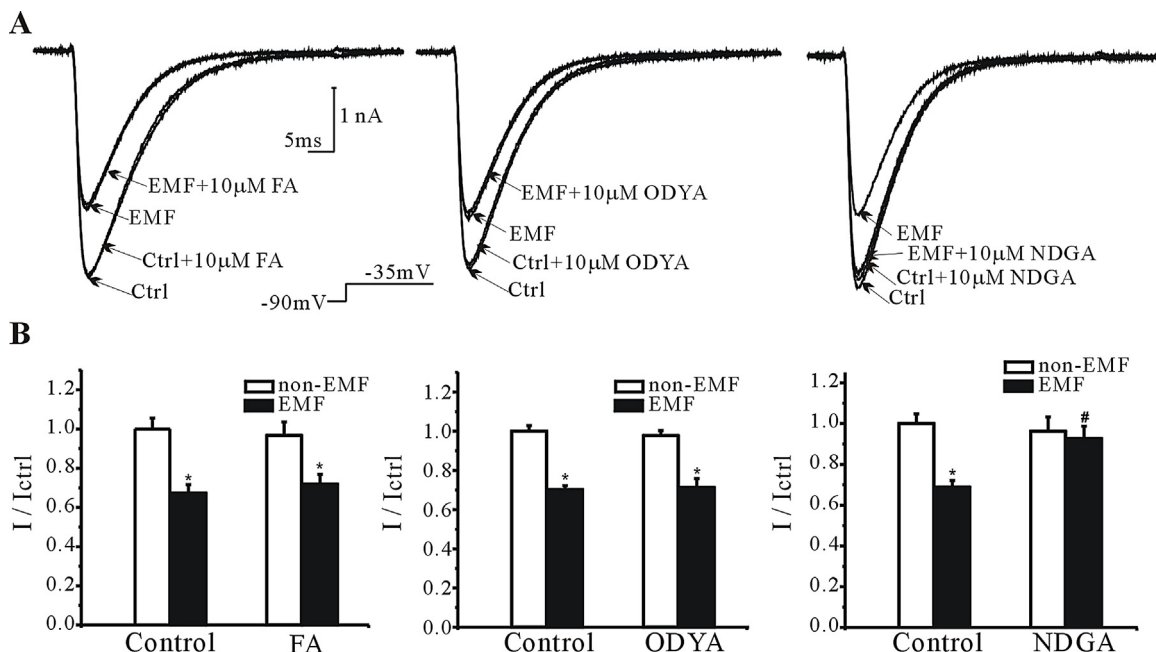


Fig. 4. The inhibition of Cav3.2 currents by ELF-EMF exposure is mediated by the lipoxygenase pathway. (A) Current traces show the effects of FA (prostaglandin endoperoxide H synthase inhibitor), ODYA (cytochromes P450 inhibitor) and NDGA (lipoxygenase inhibitor) on ELF-EMF induced inhibition of Cav3.2 channels expressed in HEK293 cells. (B) Statistical analysis of the inhibitory effects of ELF-EMF exposure on Cav3.2 channels in the present or absent of FA(left), 17-ODYA (middle) and NDGA(right). 10uM NDGA abrogated the EMF inhibition of Cav3.2 channels. Both FA and 17-ODYA did not affect the ELF-EMF inhibition of Cav3.2 channels significantly. * $P < 0.05$ compared to non-EMF control using Students' *t*-test. # $P < 0.05$ compared to the EMF-exposed group without NDGA.

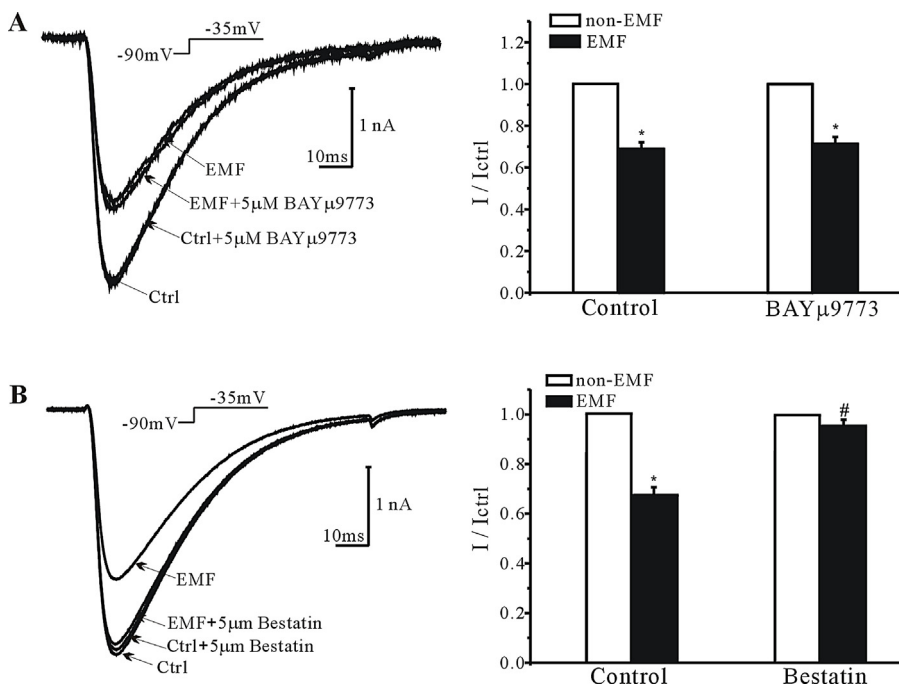


Fig. 5. The ELF-EMF inhibition of Cav3.2 channels is mediated by LTE₄. (A) The cysteinyl leukotriene receptor antagonist BAYμ.9773 did not change the inhibitory effect of ELF-EMF on Cav3.2 channels. Representative current trances were elicited by a test pulse at -35 mV from holding at -90 mV (left). Statistical analysis of the effects of BAYμ.9773 on the ELF-EMF induced inhibition of Cav3.2 channels (right). (B) Bestatin, which blocks the conversion from LTD₄ to LTE₄, abrogated the ELF-EMF inhibition of Cav3.2 channels. Currents show ELF-EMF effect on Cav3.2 currents in the presence of bestatin (left). Bar graph plots of means ± S.E.M. of normalized Cav3.2 current density (right). *P<0.05 compared to non-EMF control. #P<0.05 compared to the EMF-exposed group without bestatin.

groups. Multiple comparisons were analyzed using a one-way analysis of variance (ANOVA) followed by the post hoc Tukey test.

3. Results

3.1. Extremely low-frequency electromagnetic fields (ELF-EMF) inhibits Cav3.2 channel currents

Cav3.2 currents were elicited by a 40-ms depolarizing pulse to -35 mV from a holding potential of -90 mV at 10 s intervals. ELF-EMF (50 Hz, 0.2 mT) exposure inhibited Cav3.2 currents in a time-dependent manner (percent inhibition: 0.5 h EMF: 11 ± 2.1%, n = 45; 1 h EMF: 31.1 ± 4.71%, n = 65; 2 h EMF: 4.3 ± 2.4%, n = 60; 3 h EMF: 3.7 ± 2.3%, n = 52; Fig. 1A and B). The inhibitory effect reached a maximum at about 1 h, so we used 1 h ELF-EMF (0.2 mT) exposure for all of the following experiments. ELF-EMF decreased Cav3.2 channel currents at all voltages (Fig. 1C and D). The current–voltage (I–V) relationship was elicited by a step protocol (holding at -90 mV, depolarizing in 5-mV steps from -60 to +25 mV at 10-s intervals). We tested whether ELF-EMF inhibited Cav3.2 channels through altering the steady-state activation and inactivation of Cav3.2 channel currents. As shown in Fig. 2, exposure to ELF-EMF did not change either the steady-state activation (control: V_{1/2} = -45.1 ± 0.6 mV, n = 20; EMF: V_{1/2} = -45.3 ± 0.2 mV, n = 20, P > 0.05, Fig. 2A) or inactivation (control: V_{1/2} = -65.1 ± 0.5 mV, n = 20; EMF: V_{1/2} = -65.2 ± 0.4 mV, n = 20, P > 0.05, Fig. 2B) kinetics of Cav3.2 channel currents. We then studied whether ELF-EMF exposure inhibited Cav3.2 currents by changing protein expression. Western blot results showed that 1 h exposure to ELF-EMF (0.2 mT) did not alter Cav3.2 channel expression (EMF: 2.67 ± 3.91%, n = 4, P > 0.05 compared to control, Fig. 2C).

3.2. The ELF-EMF inhibition of Cav3.2 currents is abrogated by blocking arachidonic acid (AA) increase

AA has been shown to inhibit Cav3.2 channels [27], and a recent study reports that 50 Hz ELF-EMF increases intracellular AA concentration of rat cerebellar granule cells [26]. Therefore, we tested whether the ELF-EMF inhibition of Cav3.2 channels was mediated via increasing AA. As shown in Fig. 3A, ELF-EMF exposure increased AA concentration in HEK293 cells in a time dependent manner (0.5 h: 8.0 ± 0.8%; 1 h: 17.9 ± 3.4%; 2 h: 3.3 ± 4.1%; 3 h: 1.7 ± 2.1%, n = 3). The phospholipase A2 inhibitor CAY10502, which inhibits AA release from the phospholipid pools, abrogated ELF-EMF (1 h) induced AA increase (EMF: 17.9 ± 3.4%; EMF + CAY10502: 3.6 ± 2.7%, P < 0.05, Fig. 3B) and the ELF-EMF inhibitory effect of Cav3.2 channels (EMF: 35.7 ± 4.9%, n = 48; EMF + CAY10502: 8.9 ± 5.4%, n = 48; P < 0.05, Fig. 3C and D), which indicated that ELF-EMF exposure inhibited Cav3.2 channels through AA signaling pathway. AA shifts the steady-state inactivation of Cav3.2 currents [27], however, ELF-EMF exposure did not change either steady-state voltage activation or inactivation of Cav3.2 currents (Fig. 2). Therefore, we speculated that ELF-EMF might inhibit Cav3.2 channels by downstream metabolites of AA.

3.3. The ELF-EMF inhibition of Cav3.2 channels is mediated by LTE₄

AA has three major downstream signaling pathways which were mediated by the prostaglandin endoperoxide H synthase (PGHS), lipoxygenase (LOX) and cytochromes P450 respectively [28,29]. We used FA, NDGA and ODYA to block the above three enzymes respectively. FA, ODYA and NDGA per se had no effect on Cav3.2 channels (Fig. 4). FA and ODYA did not alter the inhibitory effect of ELF-EMF on Cav3.2 channels (EMF: 31.6 ± 4.2%, n = 36; EMF + FA: 28.2 ± 5.1%,

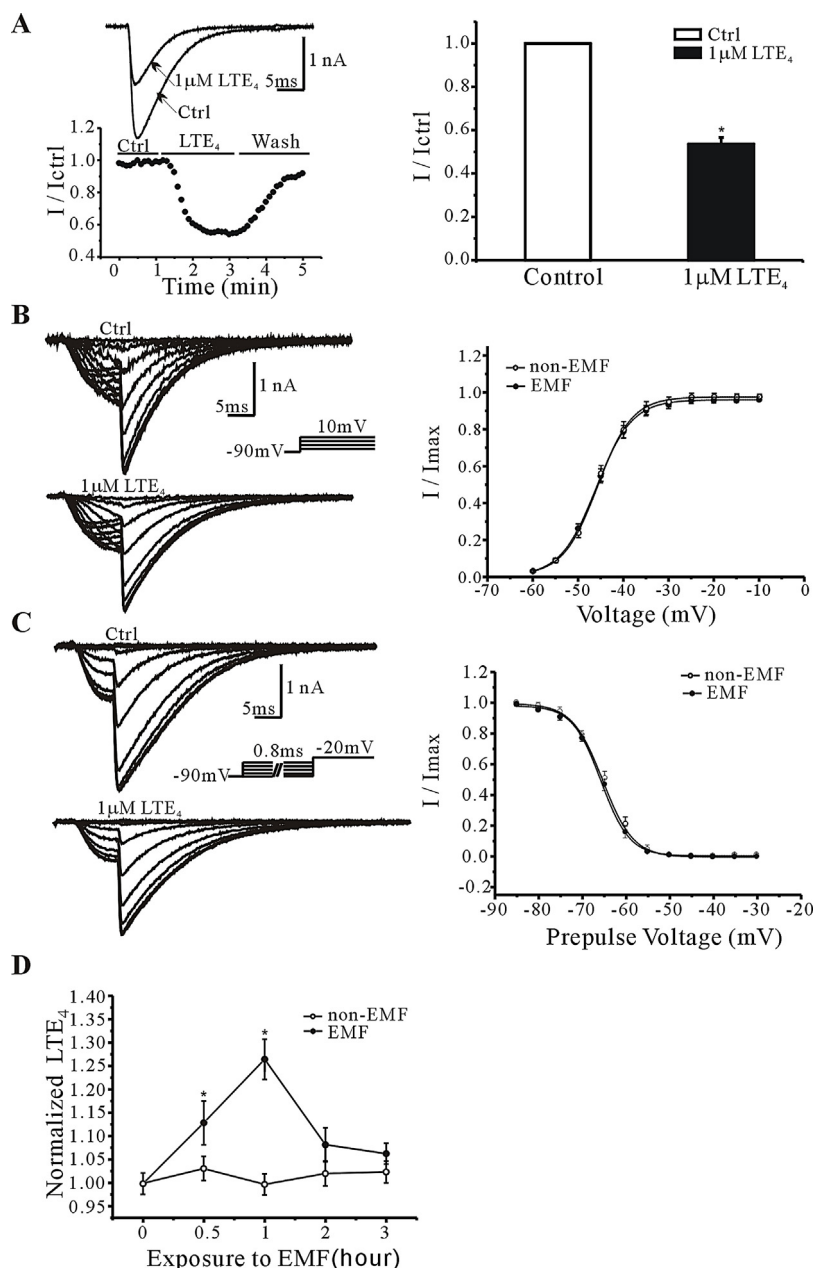


Fig. 6. LTE4 replicates the inhibitory effect of ELF-EMF on Cav3.2 channels. (A) Representative current traces show the inhibitory effect of exogenous LTE₄ on Cav3.2 channels (top left). The time course of the Cav3.2 current inhibition by 1 μM LTE₄ (bottom left). Statistical analysis of the effect of exogenous LTE₄ on I_{Ca} . The data are reported as the means ± S.E.M. from 7 cells (right). *P < 0.05 compared to control. (B) 1 μM LTE₄ did not alter the steady-state activation property of Cav3.2 currents (right). Representative currents with/without LTE4 shown to the left. (C) 1 μM LTE₄ did not alter the steady-state inactivation kinetics of Cav3.2 currents (right). Representative currents with/without LTE4 shown to the left. (D) ELF-EMF exposure increased LTE₄ release in a time-dependent manner. The data are from 4 independent experiments. *P < 0.05 compared to non-EMF control.

$n=36$; EMF+ODYA: $28.7 \pm 4.5\%$, $n=34$, $P>0.05$, Fig. 4A and B). However, 10 μM NDGA completely diminished the ELF-EMF inhibition of Cav3.2 channels (EMF: $31.1 \pm 3.1\%$, $n=38$; EMF+NDGA: $7.4 \pm 6.1\%$, $n=38$, $P<0.05$, Fig. 4A and B), which suggested that ELF-EMF exposure inhibited Cav3.2 channels through LOX-mediated signaling pathway. Through LOX pathway, AA is converted to leukotriene C₄ (LTC₄), leukotriene D₄ (LTD₄) and leukotriene E₄ (LTE₄) finally by successive enzymatic conversions [30–32]. We next investigated which metabolite of AA inhibited Cav3.2 channels.

So far, there are only two cysteinyl leukotriene receptors (CysLT1 and CysLT2) identified, which have high affinity for LTC₄ and LTD₄ binding, but have little affinity for LTE₄ [33,34].

BAYμ9773, a non-selective antagonist for both CysLT1 and CysLT2, did not change the inhibitory effect of ELF-EMF on Cav3.2 channels (EMF: $31.6 \pm 3.1\%$, $n=40$; EMF+BAYμ9773: $28.9 \pm 3.3\%$, $n=40$, $P>0.05$, Fig. 5A). Bestatin, which blocks the conversion from LTD₄ to LTE₄, was used to test whether the ELF-EMF inhibition of Cav3.2 channel currents was mediated by LTE₄. 5 μM bestatin totally abrogated the ELF-EMF inhibition of Cav3.2 channels (EMF: $31.8 \pm 2.7\%$, $n=36$; Emf+bestatin: $6.02 \pm 2.1\%$, $n=36$, $P<0.05$, Fig. 5B). The above data demonstrated that ELF-EMF exposure inhibited Cav3.2 channels via LTE₄ instead of LTC₄ and LTD₄. We next asked whether exogenous LTE₄ could inhibit Cav3.2 channels, and whether ELF-EMF could increase LTE₄ production. As shown in Fig. 6, 1 μM LTE₄ inhibited Cav3.2 channels

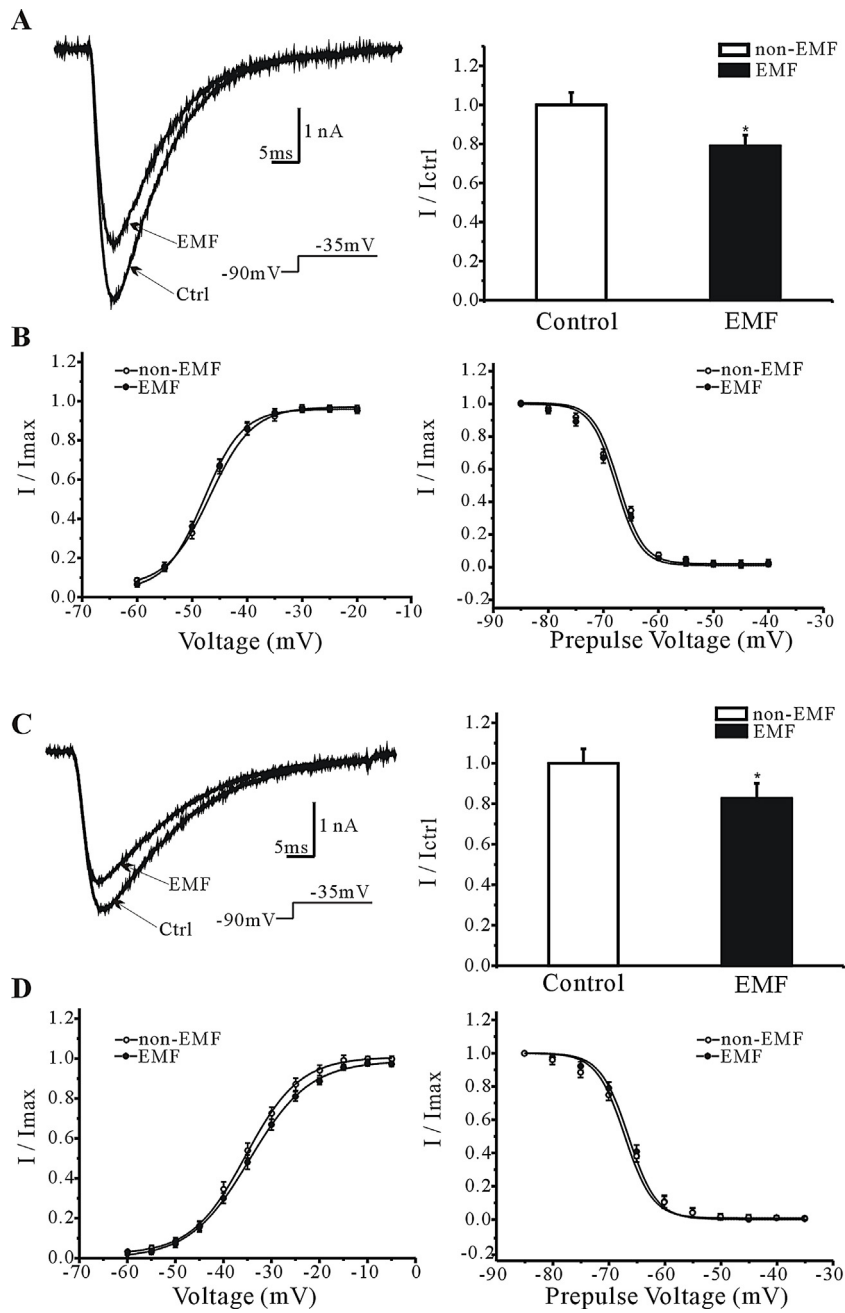


Fig. 7. ELF-EMF (50 Hz, 0.2 mT) inhibits both Cav3.1 and Cav3.3 channels. (A) Effect of exposure to ELF-EMF (1 h) on the Cav3.1 channels expressed in HEK293 cells. Sample current traces shown ELF-EMF inhibition of Cav3.1 current (left); Statistical analysis of the effect of ELF-EMF exposure on Cav3.1 channels (right). The data are reported as means \pm S.E.M. from 48 cells. * P < 0.05 compared to non-EMF control. (B) Exposure to ELF-EMF did not alter the steady-state activation (left) and inactivation (right) curves of Cav3.1 currents. (C) Effect of ELF-EMF exposure (1 h) on Cav3.3 channels. Sample current traces shown ELF-EMF inhibition of Cav3.3 current (left); Statistical analysis of the effect of ELF-EMF exposure on Cav3.3 channels (right). The data are reported as means \pm S.E.M. from 45 cells. * P < 0.05 compared to non-EMF control. (D) Exposure to ELF-EMF did not alter the steady-state activation (left) and inactivation (right) curves of Cav3.3 currents.

by $46.4 \pm 3\%$, and LTE₄ did not alter the steady-state activation (control: $V_{1/2} = -44.9 \pm 0.3$ mV, $n = 6$; LTE₄: $V_{1/2} = -45.1 \pm 0.3$ mV, $n = 6$, Fig. 6B) and inactivation (control: $V_{1/2} = -65.2 \pm 0.3$ mV, $n = 7$; LTE₄: $V_{1/2} = -65.6 \pm 0.5$ mV, $n = 7$, $P > 0.05$, Fig. 6C) properties of Cav3.2 currents. The inhibitory effect of LTE₄ on I_{Ca} began quickly and reached a maximum effect within 2 min. The inhibition was reversible within 2–3 min (Fig. 6A). ELF-EMF exposure increased LTE₄ release from HEK293 cells in a time dependent manner (0.5 h: $12.3 \pm 2.4\%$; 1 h: $25.2 \pm 4.1\%$; 2 h: $7.9 \pm 3.5\%$; 3 h: $6.1 \pm 2.1\%$, Fig. 6D), which was consistent with the ELF-EMF inhibition of Cav3.2 channels.

3.4. ELF-EMF exposure inhibits Cav3.1 and Cav3.3 channels via LTE₄

The above results demonstrated that ELF-EMF exposure inhibited Cav3.2 channels via AA/LTE₄ signaling pathway. We next tested whether ELF-EMF (50 Hz, 0.2 mT) exposure has similar inhibitory effects on Cav3.1/3.3 channels in HEK293 cells. As shown in Fig. 7, 1 h ELF-EMF (0.2 mT) exposure inhibited Cav3.1/3.3 channels significantly (percent inhibition, Cav3.1: $21 \pm 5.4\%$, $n = 48$; Cav3.3: $17.6 \pm 7.4\%$, $n = 45$; $P < 0.05$, compared to control, Fig. 7A and B). Exposure to ELF-EMF did not alter the steady-state activation

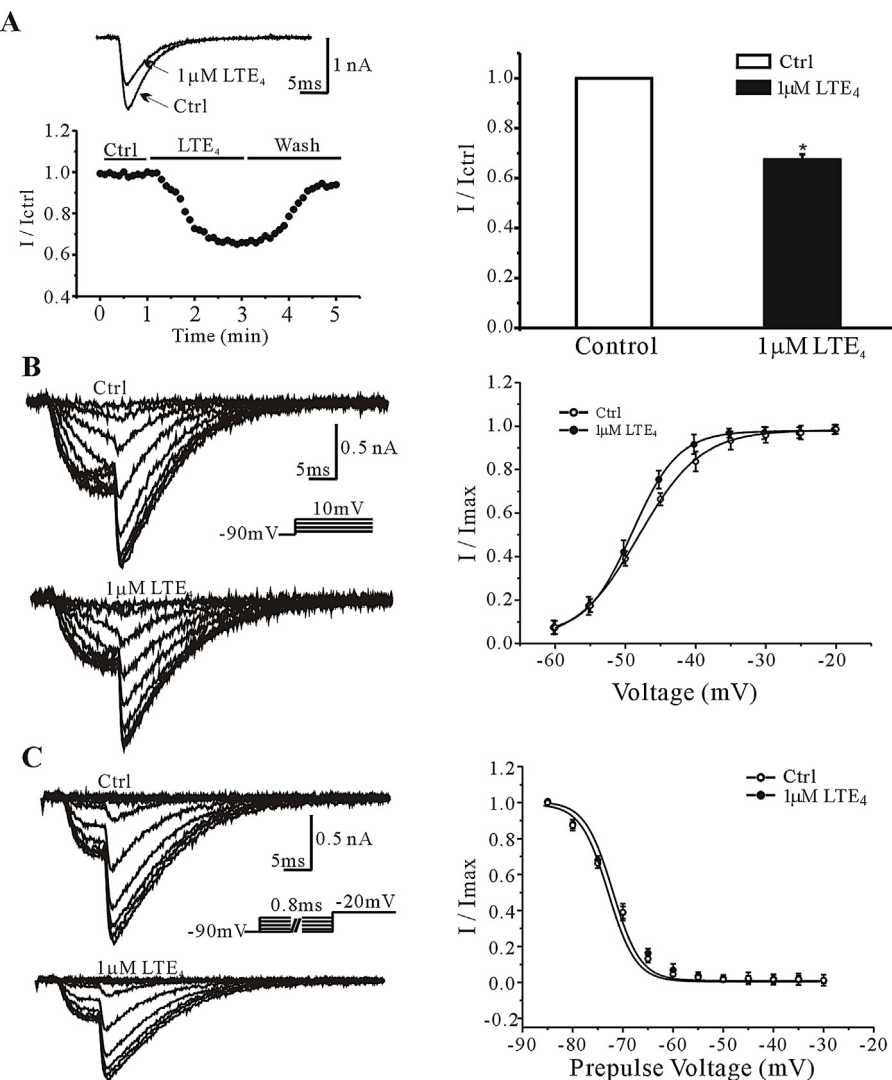


Fig. 8. Exogenous LTE₄ mimics the ELF-EMF inhibition of Cav3.1 channels. (A) Sample current traces show the effect of the extracellular applying of 1 μM LTE₄ on Cav3.1 channels expressed in HEK293 cells (top left). The time course of the Cav3.1 current inhibition by 1 μM LTE₄ (bottom left). Statistical analysis of the effects of 1 μM LTE₄ on Cav3.1 channels (right). *P < 0.05 compared to control. (B) 1 μM LTE₄ did not change the steady-state activation curve of Cav3.1 currents (right); Sample current traces with/without LTE₄ shown to the left. (C) 1 μM LTE₄ did not alter the steady-state inactivation curve of Cav3.1 currents (right); Sample current traces with/without LTE₄ shown to the left.

and inactivation kinetics of Cav3.1 channels (activation, control: $V_{1/2} = -46.3 \pm 0.6$; EMF: $V_{1/2} = -47.3 \pm 0.3$; $n = 18$, $P > 0.05$; inactivation, control: $V_{1/2} = -68.2 \pm 0.4$; EMF: $V_{1/2} = -68.7 \pm 0.3$; $n = 18$, $P > 0.05$, Fig. 7B). Exposure to ELF-EMF also did not change the steady-state activation and inactivation properties of Cav3.3 channels (activation, control: $V_{1/2} = -35.4 \pm 0.2$; EMF: $V_{1/2} = -34.6 \pm 0.3$; $n = 17$, $P > 0.05$; inactivation, control: $V_{1/2} = -67.1 \pm 0.2$; EMF: $V_{1/2} = -66.4 \pm 0.3$; $n = 17$, $P > 0.05$, Fig. 7D). We then tested whether exogenous LTE₄ could mimic the ELF-EMF inhibitory effects on Cav3.1/3.3 channels.

Exogenous LTE₄ inhibited Cav3.1 channels ($32.5 \pm 2\%$, $n = 7$, $P < 0.05$, compared to control Fig. 8A) and did not alter the steady-state activation (control: $V_{1/2} = -48.1 \pm 0.2$ mV, $n = 7$; LTE₄: $V_{1/2} = -48.8 \pm 0.1$ mV, $n = 7$; $P > 0.05$, Fig. 8B) and inactivation (control: $V_{1/2} = -72.2 \pm 0.1$ mV, $n = 7$; LTE₄: $V_{1/2} = -72.1 \pm 0.1$ mV, $n = 7$; $P > 0.05$, Fig. 8C) of Cav3.1 currents. LTE₄ inhibited Cav3.3 channels significantly ($34.3 \pm 6.6\%$, $n = 7$, $P < 0.05$, compared to control, Fig. 9A), and did not change the steady-state activation (control: $V_{1/2} = -35.8 \pm 0.2$ mV, $n = 7$; LTE₄: $V_{1/2} = -34 \pm 0.2$ mV, $n = 7$, $P > 0.05$, Fig. 9B) and inactivation (control: $V_{1/2} = -67.4 \pm 0.3$ mV,

$n = 7$; LTE₄: $V_{1/2} = -66.5 \pm 0.3$ mV, $n = 7$, $P > 0.05$, Fig. 9C) kinetics of Cav3.3 currents. The above data suggested that ELF-EMF exposure inhibited Cav3.1, Cav3.2 and Cav3.3 channels in a similar way.

3.5. ELF-EMF exposure inhibits native T-type calcium channels in mouse cortical neurons via LTE₄

The primary cultured cortical neurons were used to test whether ELF-EMF exposure inhibits native T-type channel currents via LTE₄ pathway. The native T-type calcium channel currents in cortical neurons were elicited by a 40-ms depolarizing pulse to -40 mV from a holding potential of -90 mV at 10 s intervals. In order to avoid any contribution of HVA currents, the 100 μM Ni²⁺ was used to confirm the T-type Ca²⁺ currents. Ni²⁺-sensitive Ca²⁺ currents ($I_{\text{control}} - I_{\text{Ni}^{2+}}$) were used to calculate the ELF-EMF effect on T-type channels. As shown in Fig. 10A, one hour exposure to ELF-EMF (50 Hz, 0.2 mT) inhibits Ni²⁺ sensitive T-type Ca²⁺ currents significantly in mouse cortical neurons. Bestatin, which blocks the conversion from LTD4 to LTE₄, abrogated the ELF-EMF inhibition of T-type Ca²⁺ currents (EMF: $25.2 \pm 1.6\%$, $n = 35$; EMF + bestatin:

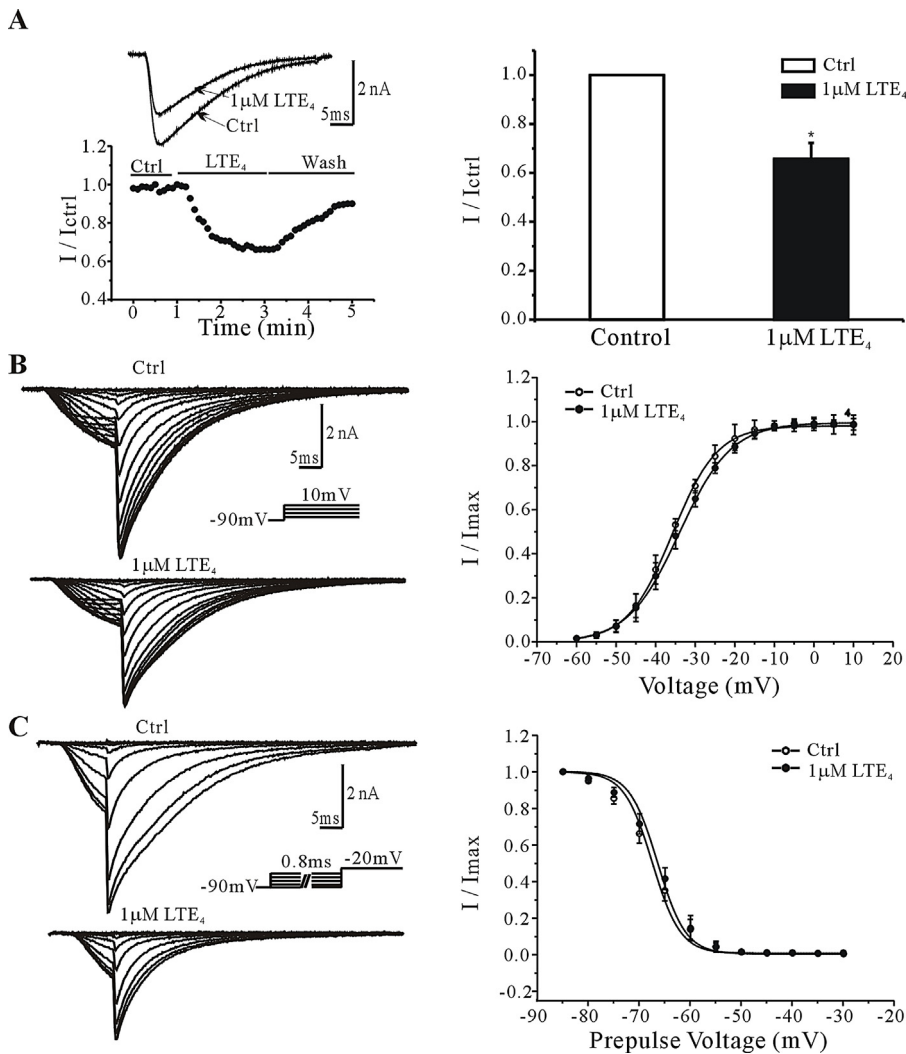


Fig. 9. Exogenous LTE₄ mimics the ELF-EMF inhibitory effect on Cav3.3 channels. (A) Representative current traces show the inhibitory effect of exogenous LTE₄ on Cav3.3 channels expressed in HEK293 cells (top left). The time course of the Cav3.3 current inhibition by 1 μM LTE₄ (bottom left). Statistical analysis of the effect of 1 μM LTE₄ on Cav3.3 currents (right). *P < 0.05 compared to control. (B) 1 μM LTE₄ did not change the steady-state activation curve of Cav3.3 currents (right); Sample current traces with/without LTE₄ shown to the left. (C) 1 μM LTE₄ did not alter the steady-state inactivation curve of Cav3.3 currents (right); Sample current traces with/without LTE₄ shown to the left.

9.1 ± 5.9%, n = 32, P < 0.05, Fig. 10B). Exogenous LTE₄ inhibited native T-type channel currents by 46.4 ± 5.9% (n = 5, Fig. 10C and D). The data above suggested that ELF-EMF inhibits native T-type channel currents in cortical neurons via LTE₄ pathway.

4. Discussion

In present study, we reports that exposure to ELF-EMF (50 Hz, 0.2 mT) inhibited cloned T-type calcium channels expressed in HEK293 cells via AA/LTE₄ signaling pathway. Among T-type channels, ELF-EMF preferentially inhibits Cav3.2 channels (Figs. 1 and 7). Correspondingly, LTE₄ has a greater inhibitory effect on Cav3.2 channels than Cav3.1 and Cav3.3 channels (Figs. 6A, 8A and 9A).

It has been well documented that increased L-type channel activity is involved in various ELF-EMF induced biological effects. Surprisingly, we find that ELF-EMF exposure inhibits T-type calcium channels. In agree with the previous report [26], exposure to ELF-EMF (50 Hz) increases AA level in HEK293 cell. Exogenous AA directly inhibits T-type calcium channels via shifting inactivation curve to more negative potential [27,35,36]. Blocking ELF-EMF induced AA increase abrogated the ELF-EMF inhibition of Cav3.2 channels (Fig. 3). However, ELF-EMF did not change the

steady-state inactivation kinetics of T-type channels (Fig. 2), and NDGA, which blocks LOX pathway of AA, completely diminished the ELF-EMF inhibition of Cav3.2 channels (Fig. 4). These data suggest that ELF-EMF inhibition of T-type calcium channels is mediated by metabolites of AA instead of AA direct effect.

Through LOX pathway, AA is finally converted to the cysteinyl leukotrienes (cys-LTs) including LTC₄, LTD₄ and LTE₄. So far, There are only two cysteinyl leukotriene receptors (CysLT1 and CysLT2) identified, which have high affinity for LTC₄ and LTD₄ binding, but have little affinity for LTE₄ [33,34]. A number of studies show that LTE₄ regulate various biological functions independent of CysLT1/CysLT2 receptors, indicating the existence of unknown cysteinyl leukotriene receptor/receptors for LTE₄ [37–40]. Our results show that the CysLT1/CysLT2 receptor inhibitor BAYu9773 did not change the ELF-EMF inhibitory effect on Cav3.2 channels (Fig. 5A), and that blocking the conversion of LTD₄ to LTE₄ abrogated the ELF-EMF inhibition of Cav3.2 channels (Fig. 5B). The data suggest that ELF-EMF inhibition of Cav3.2 channels is mediated by LTE₄, but not via classic CysLT1/CysLT2 receptors. The mechanism of LTE₄ inhibition of T-type calcium channels need to be investigated further. Cys-LTs are highly potent mediators of inflammation, and play a key role in

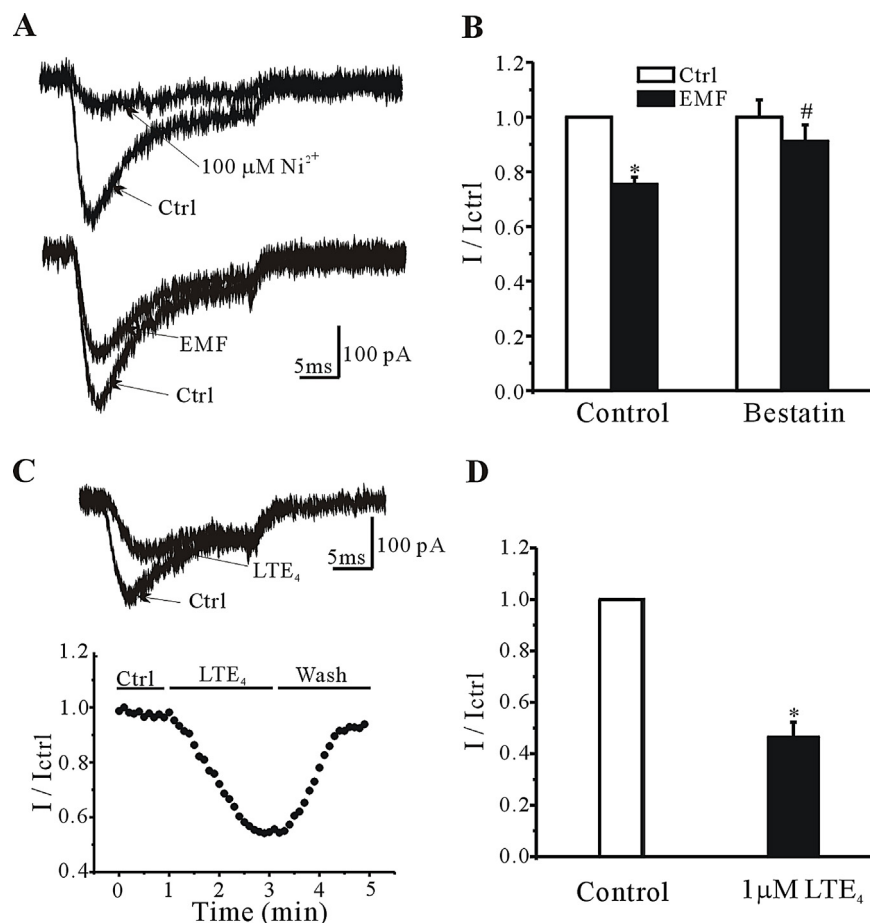


Fig. 10. ELF-EMF exposure inhibits native T-type calcium channels in mouse cortical neurons via LTE₄. (A) Representative current traces show the native Ni^{2+} sensitive T-type Ca^{2+} currents in mouse cortical neurons (top). The native T-type Ca^{2+} currents were elicited by a 40-ms depolarizing pulse to -40 mV from a holding potential of -90 mV . Sample current traces shown ELF-EMF inhibition of T-type Ca^{2+} currents in mouse cortical neurons (bottom). (B) Bestatin abrogated the ELF-EMF inhibition of T-type Ca^{2+} currents in cortical neurons. Bar graph plots of means \pm S.E.M. of normalized T-type Ca^{2+} currents. * $P < 0.05$ compared to non-EMF control. # $P < 0.05$ compared to the EMF-exposed group without bestatin. (C) Representative current traces show the inhibitory effect of exogenous LTE₄ on native T-type calcium channels in mouse cortical neurons (top). The time course of T-type Ca^{2+} current inhibition by 1 μM LTE₄ (bottom). (D) Statistical analysis of the effect of 1 μM LTE₄ on T-type Ca^{2+} current. * $P < 0.05$ compared to control.

asthma [41,42]. Urinary LTE₄ has been used as a predictor of risk for asthma in clinical study [43]. Exposure to ELF-EMF increases LTE₄ lever (Fig. 6D), which may provide a possible molecular explanation for the previous epidemiological report that EMF exposure could be a risk factor for asthma [44]. The ELF-EMF induced increases of both AA and LTE₄ are time dependent, reaching maximum levels at about 1 h and disappeared after 2 h (Figs. 3A and 6D). That may explain the biphasic inhibition of ELF-EMF exposure on T-type channel currents (Fig. 1).

The primary cultured mouse cortical neurons were used to test whether ELF-EMF exposure inhibits native T-type channel currents. Mouse cortical neurons express both HVA and LVA calcium channels. We used low depolarization voltage (-40 mV) to avoid activation of HVA calcium channels, and used Ni^{2+} to further confirm that the recorded Ca^{2+} currents were form LVA channels (Fig. 10A). Our data show that 1 h ELF-EMF (50 Hz, 0.2 mT) exposure inhibits native T-type channel currents in mouse cortical neurons via LTE₄ pathway.

In conclusion, our results provide the first evidence that exposure to ELF-EMF increases LTE₄ release, and that ELF-EMF exposure inhibits cloned human T-type calcium channels expressed in HEK293 cells and native T-type channel currents in mouse cortical neurons via AA/LTE₄ signaling pathway.

Conflict of interest

The authors declare no conflicts of interest.

Acknowledgements

The authors would like thank Dr. Edward Perez-Reyes and Dr. Paula Barrett for providing the human Cav3.x constructs. This work was supported by the grants from the National Basic Research Program of China (2011CB503703), National Natural Science Foundation of China (NSFC 310000515 and NSFC 31271240) and The Shanghai Leading Academic Discipline Project [B111].

References

- [1] M.T. Santini, G. Rainaldi, P.L. Indovina, Cellular effects of extremely low frequency (ELF) electromagnetic fields, International journal of radiation biology 85 (2009) 294–313.
- [2] D.A. McNamee, A.G. Legros, D.R. Krewski, G. Wisenberg, F.S. Prato, A.W. Thomas, A literature review: the cardiovascular effects of exposure to extremely low frequency electromagnetic fields, International Archives of Occupational and Environmental Health 82 (2009) 919–933.
- [3] A. Maes, L. Verschaeve, Can cytogenetics explain the possible association between exposure to extreme low-frequency magnetic fields and Alzheimer's disease? Journal of Applied Toxicology: JAT 32 (2012) 81–87.

- [4] J. Wallczek, Electromagnetic field effects on cells of the immune system: the role of calcium signaling, *FASEB Journal: Official Publication of the Federation of American Societies for Experimental Biology* 6 (1992) 3177–3185.
- [5] R. Hemmersbach, E. Becker, W. Stockem, Influence of extremely low frequency electromagnetic fields on the swimming behavior of ciliates, *Bioelectromagnetics* 18 (1997) 491–498.
- [6] C. Aldinucci, M. Palmi, G. Sgaragli, A. Benocci, A. Meini, F. Pessina, G.P. Pessina, The effect of pulsed electromagnetic fields on the physiologic behaviour of a human astrocytoma cell line, *Biochimica et Biophysica Acta* 1499 (2000) 101–108.
- [7] R. Tonini, M.D. Baroni, E. Masala, M. Micheletti, A. Ferroni, M. Mazzanti, Calcium protects differentiating neuroblastoma cells during 50 Hz electromagnetic radiation, *Biophysical Journal* 81 (2001) 2580–2589.
- [8] H.J. Kim, J. Jung, J.H. Park, J.H. Kim, K.N. Ko, C.W. Kim, Extremely low-frequency electromagnetic fields induce neural differentiation in bone marrow derived mesenchymal stem cells, *Experimental Biology and Medicine* 238 (2013) 923–931.
- [9] C. Morabito, F. Rovetta, M. Bizzarri, G. Mazzoleni, G. Fano, M.A. Mariggio, Modulation of redox status and calcium handling by extremely low frequency electromagnetic fields in C2C12 muscle cells: A real-time, single-cell approach, *Free Radical Biology & Medicine* 48 (2010) 579–589.
- [10] R. Gaetani, M. Ledda, L. Barile, I. Chimenti, F. De Carlo, E. Forte, V. Ionta, L. Giuliani, E. D'Emilia, G. Frati, F. Miraldo, D. Pozzi, E. Messina, S. Grimaldi, A. Giacomello, A. Lisi, Differentiation of human adult cardiac stem cells exposed to extremely low-frequency electromagnetic fields, *Cardiovascular Research* 82 (2009) 411–420.
- [11] M.L. Pall, Electromagnetic fields act via activation of voltage-gated calcium channels to produce beneficial or adverse effects, *Journal of Cellular and Molecular Medicine* (2013).
- [12] W.A. Catterall, E. Perez-Reyes, T.P. Snutch, J. Striessnig, International Union of Pharmacology. XLVIII. Nomenclature and structure-function relationships of voltage-gated calcium channels, *Pharmacological Reviews* 57 (2005) 411–425.
- [13] L. Verdugo-Díaz, T. Olivares-Banuelos, L. Navarro, R. Drucker-Colin, Effects of extremely low frequency electromagnetic field stimulation on cultured chromaffin cells, *Annals of the New York Academy of Sciences* 971 (2002) 266–268.
- [14] C. Grassi, M. D'Ascenzo, A. Torsello, G. Martinotti, F. Wolf, A. Cittadini, G.B. Azzena, Effects of 50 Hz electromagnetic fields on voltage-gated Ca²⁺ channels and their role in modulation of neuroendocrine cell proliferation and death, *Cell Calcium* 35 (2004) 307–315.
- [15] J.H. Jeong, C. Kum, H.J. Choi, E.S. Park, U.D. Sohn, Extremely low frequency magnetic field induces hyperalgesia in mice modulated by nitric oxide synthesis, *Life Sciences* 78 (2006) 1407–1412.
- [16] A. Lisi, M. Ledda, E. Rosola, D. Pozzi, E. D'Emilia, L. Giuliani, A. Foletti, A. Modesti, S.J. Morris, S. Grimaldi, Extremely low frequency electromagnetic field exposure promotes differentiation of pituitary corticotrope-derived AtT20 D16V cells, *Bioelectromagnetics* 27 (2006) 641–651.
- [17] R. Piacentini, C. Ripoli, D. Mezzogori, G.B. Azzena, C. Grassi, Extremely low-frequency electromagnetic fields promote in vitro neurogenesis via upregulation of Ca(v)1-channel activity, *Journal of Cellular Physiology* 215 (2008) 129–139.
- [18] B. Cuccuruzzo, L. Leone, M.V. Podda, R. Piacentini, E. Riccardi, C. Ripoli, G.B. Azzena, C. Grassi, Exposure to extremely low-frequency (50 Hz) electromagnetic fields enhances adult hippocampal neurogenesis in C57BL/6 mice, *Experimental Neurology* 226 (2010) 173–182.
- [19] E. Perez-Reyes, Molecular physiology of low-voltage-activated t-type calcium channels, *Physiological Reviews* 83 (2003) 117–161.
- [20] J.R. Huguenard, Low-threshold calcium currents in central nervous system neurons, *Annual Review of Physiology* 58 (1996) 329–348.
- [21] G. Santoni, M. Santoni, M. Nabissi, Functional role of T-type calcium channels in tumour growth and progression: prospective in cancer therapy, *British Journal of Pharmacology* 166 (2012) 1244–1246.
- [22] S.M. Cain, T.P. Snutch, T-type calcium channels in burst-firing, network synchrony, and epilepsy, *Biochimica et Biophysica Acta* 1828 (2013) 1572–1578.
- [23] S.D. DePuy, J. Yao, C. Hu, W. McIntire, I. Bidaud, P. Lory, F. Rastinejad, C. Gonzalez, J.C. Garrison, P.Q. Barrett, The molecular basis for T-type Ca²⁺ channel inhibition by G protein beta2gamma2 subunits, *Proceedings of the National Academy of Sciences of the United States of America* 103 (2006) 14590–14595.
- [24] J.C. Gomora, J. Murbartian, J.M. Arias, J.H. Lee, E. Perez-Reyes, Cloning and expression of the human T-type channel Ca(v)3.3: insights into prepulse facilitation, *Biophysical Journal* 83 (2002) 229–241.
- [25] Y.L. He, C.L. Zhang, X.F. Gao, J.J. Yao, C.L. Hu, Y.A. Mei, Cyproheptadine enhances the I(K) of mouse cortical neurons through sigma-1 receptor-mediated intracellular signal pathway, *PLoS One* 7 (2012) e41303.
- [26] Y.L. He, D.D. Liu, Y.J. Fang, X.Q. Zhan, J.J. Yao, Y.A. Mei, Exposure to extremely low-frequency electromagnetic fields modulates Na⁺ currents in rat cerebellar granule cells through increase of AA/PGE2 and EP receptor-mediated cAMP/PKA pathway, *PLoS One* 8 (2013) e54376.
- [27] Y. Zhang, L.L. Cribbs, J. Satin, Arachidonic acid modulation of alpha1H, a cloned human T-type calcium channel, *American journal of physiology, Heart and Circulatory Physiology* 278 (2000) H184–H193.
- [28] A.R. Brash, Arachidonic acid as a bioactive molecule, *The Journal of Clinical Investigation* 107 (2001) 1339–1345.
- [29] D.C. Zeldin, Epoxygenase pathways of arachidonic acid metabolism, *The Journal of Biological Chemistry* 276 (2001) 36059–36062.
- [30] C.W. Lee, R.A. Lewis, E.J. Corey, K.F. Austen, Conversion of leukotriene D4 to leukotriene E4 by a dipeptidase released from the specific granule of human polymorphonuclear leucocytes, *Immunology* 48 (1983) 27–35.
- [31] B.K. Lam, J.F. Penrose, G.J. Freeman, K.F. Austen, Expression cloning of a cDNA for human leukotriene C4 synthase, an integral membrane protein conjugating reduced glutathione to leukotriene A4, *Proceedings of the National Academy of Sciences of the United States of America* 91 (1994) 7663–7667.
- [32] B.Z. Carter, Z.Z. Shi, R. Barrios, M.W. Lieberman, gamma-glutamyl leukotrienase, a gamma-glutamyl transpeptidase gene family member, is expressed primarily in spleen, *The Journal of Biological Chemistry* 273 (1998) 28277–28285.
- [33] K.R. Lynch, G.P. O'Neill, Q. Liu, D.S. Im, N. Sawyer, K.M. Metters, N. Coulombe, M. Abramovitz, D.J. Figueroa, Z. Zeng, B.M. Connolly, C. Bai, C.P. Austin, A. Chateauneuf, R. Stocco, G.M. Greig, S. Kargman, S.B. Hooks, E. Hosfield, D.L. Williams, A.W. Ford-Hutchinson Jr., C.T. Caskey, J.F. Evans, Characterization of the human cysteinyl leukotriene CysLT1 receptor, *Nature* 399 (1999) 789–793.
- [34] C.E. Heise, B.F. O'Dowd, D.J. Figueroa, N. Sawyer, T. Nguyen, D.S. Im, R. Stocco, J.N. Bellefeuille, M. Abramovitz, R. Cheng, D.L. Williams, Z. Zeng Jr., Q. Liu, L. Ma, M.K. Clements, N. Coulombe, Y. Liu, C.P. Austin, S.R. George, G.P. O'Neill, K.M. Metters, K.R. Lynch, J.F. Evans, Characterization of the human cysteinyl leukotriene 2 receptor, *The Journal of Biological Chemistry* 275 (2000) 30531–30536.
- [35] J. Chemin, J. Nargeot, P. Lory, Chemical determinants involved in anandamide-induced inhibition of T-type calcium channels, *The Journal of Biological Chemistry* 282 (2007) 2314–2323.
- [36] K. Talavera, M. Staes, A. Janssens, G. Droogmans, B. Nilius, Mechanism of arachidonic acid modulation of the T-type Ca²⁺ channel alpha1G, *The Journal of General Physiology* 124 (2004) 225–238.
- [37] S. Paruchuri, Y. Jiang, C. Feng, S.A. Francis, J. Plutzky, J.A. Boyce, Leukotriene E4 activates peroxisome proliferator-activated receptor gamma and induces prostaglandin D2 generation by human mast cells, *The Journal of Biological Chemistry* 283 (2008) 16477–16487.
- [38] A. Maekawa, Y. Kanaoka, W. Xing, K.F. Austen, Functional recognition of a distinct receptor preferential for leukotriene E4 in mice lacking the cysteinyl leukotriene 1 and 2 receptors, *Proceedings of the National Academy of Sciences of the United States of America* 105 (2008) 16695–16700.
- [39] Y. Nonaka, T. Hiramoto, N. Fujita, Identification of endogenous surrogate ligands for human P2Y12 receptors by *in silico* and *in vitro* methods, *Biochemical and Biophysical Research Communications* 337 (2005) 281–288.
- [40] S. Paruchuri, H. Tashiro, C. Feng, A. Maekawa, W. Xing, Y. Jiang, Y. Kanaoka, P. Conley, J.A. Boyce, Leukotriene E4-induced pulmonary inflammation is mediated by the P2Y12 receptor, *The Journal of Experimental Medicine* 206 (2009) 2543–2555.
- [41] T.M. Laidlaw, J.A. Boyce, Cysteinyl leukotriene receptors, old and new; implications for asthma, *Clinical and Experimental Allergy: Journal of the British Society for Allergy and Clinical Immunology* 42 (2012) 1313–1320.
- [42] R.K. Singh, S. Gupta, S. Dastidar, A. Ray, Cysteinyl leukotrienes and their receptors: molecular and functional characteristics, *Pharmacology* 85 (2010) 336–349.
- [43] N. Rabinovitch, N. Reisdorff, L. Silveira, E.W. Gelfand, Urinary leukotriene E(4) levels identify children with tobacco smoke exposure at risk for asthma exacerbation, *The Journal of Allergy and Clinical Immunology* 128 (2011) 323–327.
- [44] D.K. Li, H. Chen, R. Odouli, Maternal exposure to magnetic fields during pregnancy in relation to the risk of asthma in offspring, *Archives of Pediatrics & Adolescent Medicine* 165 (2011) 945–950.